Stratlets: Low Reynolds Number Point-Force Solutions in a Stratified Fluid

A. M. Ardekani[1] and R. Stocker[2]

[1]*Department of Mechanical Engineering, Massachusetts Institute of Technology, Cambridge, Massachusetts 02139, USA*
[2]*Department of Civil and Environmental Engineering, Massachusetts Institute of Technology, Cambridge, Massachusetts 02139, USA*

We present fundamental solutions of low Reynolds number flows in a stratified fluid, including the case of a point force (Stokeslet) and a doublet. Stratification dramatically alters the flow by creating toroidal eddies, and velocity decays much faster than in a homogeneous fluid. The fundamental length scale is set by the competition of buoyancy, diffusion and viscosity, and is $O(100~\mu\text{m--}1~\text{mm})$ in aquatic environments. Stratification can therefore affect the swimming of small organisms and the sinking of marine snow particles, and diminish the effectiveness of mechanosensing in the ocean.

The hydrodynamics of small swimming organisms has been intensively studied for more than half a century [1,2], as microbial motility is important in a broad range of fields, with oceanographic, biomedical, industrial, and environmental applications. Because organism size (a) and speed (U) are small, swimming is characterized by low Reynolds numbers, $\text{Re} = aU/\nu \ll 1$ (where ν is the kinematic viscosity). Hence, inertial forces are negligible *vis-à-vis* viscous forces and the equation governing fluid motion (Stokes equation) is linear. Linearity has greatly facilitated analysis of the flow generated by ciliary and flagellar motion through superposition of fundamental solutions.

The most fundamental of these solutions is the flow generated by a point force, $\mathbf{f} = (f_1, f_2, f_3)$, obtained by solving the inhomogeneous Stokes equation

$$\nabla p - \mu \nabla^2 \mathbf{u} = \mathbf{f}\delta(\mathbf{r}), \qquad \nabla \cdot \mathbf{u} = 0, \qquad (1)$$

where p is the pressure, μ the dynamic viscosity, $\mathbf{u} = (u, v, w)$ the velocity, $\mathbf{r} = (x, y, z)$ the position, and $\delta(\mathbf{r})$ the delta function. The solution,

$$\mathbf{u}_{\text{Stokeslet}} = \frac{1}{8\pi\mu}\left\{\frac{\mathbf{f}}{r} + \frac{(\mathbf{f}\cdot\mathbf{r})\mathbf{r}}{r^3}\right\}, \quad p_{\text{Stokeslet}} = \frac{\mathbf{f}\cdot\mathbf{r}}{4\pi r^3}, \quad (2)$$

is known as "Stokeslet."

Derivatives of the Stokeslet are also solutions. For example, the flow generated by two equal and opposite forces (Stokes doublet) is $\mathbf{u}_{\text{doublet}} = -\boldsymbol{\beta}\cdot\nabla\mathbf{u}_{\text{Stokeslet}}$, where $\boldsymbol{\beta}$ is the pole moment vector between the two forces. The stresslet is the symmetric component of the Stokes doublet and is often used as a first-order model for a swimming microorganism, where thrust and drag forces balance. Higher-order solutions can be similarly derived [3].

Many aquatic environments are not homogeneous, but are characterized by regions of sharp vertical variation in fluid density ("pycnoclines") caused by gradients in temperature ("thermoclines") or salinity ("haloclines"). In confined environments like rock fractures or ice pores, strong density gradients can develop because mixing is often negligible [4]. In oceans and lakes, intense biological activity and accumulation of particles and organisms are

associated with pycnoclines [4]. Yet, with the exception of a drag increase on settling bodies [5,6], little is known about the effect of stratification on the motion of small living and nonliving particles. Here we present fundamental solutions for low Reynolds number flows in a stratified fluid caused by force singularities. We call this class of solutions "Stratlets."

A distinctive feature of a stratified fluid is its resistance against motion perpendicular to isopycnals (i.e., surfaces of constant density) [7]. For example, flow goes primarily around, rather than over or under, a body moving horizontally in a vertical stratification [7]. On the other hand, it remains unclear whether stratification affects the flow field of small particles and organisms, since their size [$O(\text{mm})$] is much smaller than the length scale over which density changes, ρ_0/γ [$O(\text{km})$], where ρ_0 is a reference density and γ is the background density gradient. Analysis of the stratified Stokes equation will reveal that the appropriate length scale for measuring the effects of stratification results in fact from a combination of buoyancy, diffusion and viscosity, and is indeed $O(\text{mm})$.

The steady flow induced in a vertically stratified fluid by a point force $\mathbf{f}$, of magnitude $|\mathbf{f}|$ and direction $\hat{\mathbf{f}}$, obeys

$$\rho\mathbf{u}\cdot\nabla\mathbf{u} + \nabla p - \rho\nu\nabla^2\mathbf{u} = \rho\mathbf{g} + \mathbf{f}\delta(\mathbf{r}),$$
$$\nabla\cdot\mathbf{u} = 0, \qquad \mathbf{u}\cdot\nabla\rho = \kappa\nabla^2\rho, \qquad (3)$$

where κ is the diffusivity of the stratifying agent, $\rho = \rho_0 - \gamma z + \rho'$ the fluid density, $\mathbf{g} = -g\hat{e}_3$ the acceleration of gravity, $\hat{e}_3$ the vertical unit vector (positive upwards), $p = -\rho_0 gz + \gamma gz^2/2 + p'$ the pressure, and primes denote perturbations from the background state. This assumes the density gradient is linear (i.e., γ is constant), typically a good approximation at μm-cm scales. Using the Boussinesq approximation and linearizing, one obtains

$$\nabla p' - \rho_0\nu\nabla^2\mathbf{u} = -\rho' g\hat{e}_3 + \mathbf{f}\delta(\mathbf{r}), \qquad \nabla\cdot\mathbf{u} = 0,$$
$$-w\gamma = \kappa\nabla^2\rho'. \qquad (4)$$

Taking the Fourier transform

$$
\begin{bmatrix} \mathbf{u} \\ p' \\ \rho' \end{bmatrix} = \frac{1}{8\pi^3} \int_{-\infty}^{\infty} e^{i\mathbf{k}\cdot\mathbf{r}} \begin{bmatrix} \mathbf{\Gamma(k)} \\ \Pi(\mathbf{k}) \\ R(\mathbf{k}) \end{bmatrix} d\mathbf{k} \tag{5}
$$

of Eq. (4), where $\mathbf{k} = (k_1, k_2, k_3)$ is the wave number vector and $k = |\mathbf{k}|$, yields

$$
i\Pi\mathbf{k} + \rho_0\nu k^2\mathbf{\Gamma} = -Rg\hat{e}_3 + \mathbf{f}, \qquad \mathbf{k}\cdot\mathbf{\Gamma} = 0,
$$
$$
-\gamma\mathbf{\Gamma}\cdot\hat{e}_3 = -\kappa k^2 R. \tag{6}
$$

After some algebra, one finds

$$
\mathbf{\Gamma} = \frac{\mathbf{f}}{A\mu k^2}\left(\mathbf{A} - \frac{\mathbf{k}^\dagger\mathbf{k}^\dagger}{\mathbf{k}\cdot\mathbf{k}^\dagger}\right), \qquad \Pi = -i\frac{\mathbf{f}\cdot\mathbf{k}^\dagger}{\mathbf{k}.\mathbf{k}^\dagger},
$$
$$
R = \frac{\gamma}{A\mu\kappa k^4}\frac{(f_3\mathbf{k} - k_3\mathbf{f})\cdot\mathbf{k}^\dagger}{\mathbf{k}\cdot\mathbf{k}^\dagger}, \tag{7}
$$

where $\mu = \rho_0\nu$ and

$$
\mathbf{A} = \begin{bmatrix} A & 0 & 0 \\ 0 & A & 0 \\ 0 & 0 & 1 \end{bmatrix}, \quad \mathbf{k}^\dagger = \mathbf{A}\mathbf{k}, \quad A = 1 + (Lk)^{-4}. \tag{8}
$$

This analysis shows that $L = (\mu\kappa/\gamma g)^{1/4}$ is the fundamental length scale of the problem, rather than ρ_0/γ. This significantly reduces the smallest scales of motion affected by stratification, as discussed further below. The same length scale also governs other stratified flow phenomena, including diffusion-driven flow along a slope [8] and double-diffusion in an inclined slot [9].

Using L to nondimensionalize length scales, $|\mathbf{f}|/(\mu L)$ for velocities and $|\mathbf{f}|/(gL^3)$ for densities, one can solve for the dimensionless velocity field of a stratified Stokeslet,

$$
\mathbf{u}_{\mathrm{Stokeslet}}^{S} = F^{-1}\left\{\frac{\hat{\mathbf{f}}}{k^2 A}\left(\mathbf{A} - \frac{\mathbf{k}^\dagger\mathbf{k}^\dagger}{\mathbf{k}.\mathbf{k}^\dagger}\right)\right\}, \tag{9}
$$

where S indicates "stratified", $A = 1 + k^{-4}$, and F^{-1} is the Fourier inverse, here computed numerically using the

Fast Fourier Transform. The associated dimensionless density perturbation is $\rho' = (4\pi r)^{-1} * w$, where $*$ is the convolution operator and w is vertical velocity.

The comparison between a homogeneous and a stratified Stokeslet for a vertical, downward point force shows that stratification fundamentally alters the flow field [Figs. 1(a) and 1(b)]. In a homogeneous fluid, streamlines are open and flow is everywhere downwards [Fig. 1(a)]. In a stratified fluid, recirculation regions appear, manifested by closed streamlines [Fig. 1(b)]. This is a consequence of buoyancy limiting the vertical excursion of fluid elements, resulting in the formation of a toroidal eddy around the point force. Viscous shear then transfers momentum to the adjacent fluid, setting in motion additional, progressively weaker eddies.

Eddy formation is consistent with the tendency of stratification to partially confine vertical motion. This is highlighted by a comparison with an extreme case of confinement, where we replaced stratification by two horizontal walls with no-slip boundary conditions. This also leads to the formation of an eddy [Fig. 1(c); see also [10]], which is qualitatively similar to that generated by a stratified Stokeslet [Fig. 1(b)].

By confining fluid motion, stratification affects the decay rate of the velocity field with distance r from the point force. For a homogeneous Stokeslet, velocity decays as $1/r$. Figure 2 shows the vertical velocity w^S of a stratified Stokeslet along axes x and z (where horizontal velocity is zero). The solution of the homogeneous case ($1/r$ decay) is recovered in Fig. 2(a) when $x \to 0$ (along the x axis, red dashed line) or when $z \to 0$ (along the z axis, green dashed-dotted line), since the length scale $L \to \infty$ in a homogeneous fluid. The decay rate is larger for a stratified than a homogeneous fluid [Fig. 2(a)], as emphasized by normalizing w^S with its homogeneous counterpart, w^H [Fig. 2(b)]. For example, w^S is -4% of w^H at $z = 5$. w^S/w^H goes to zero at $z = 3.8$ and at $x = 1.5$ along the coordinate axes [Fig. 2(b); red dots in Fig. 1(b)], providing estimates for the main eddy's height and radius.
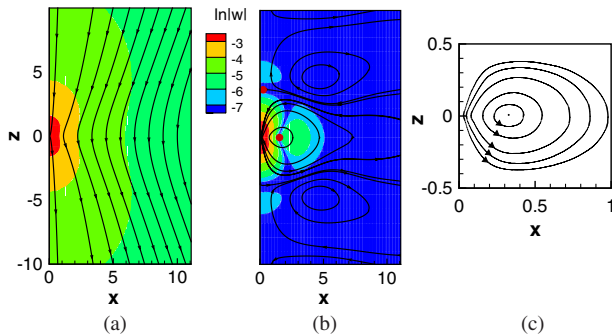

FIG. 1 (color online).   Flow induced by a vertical downward Stokeslet in (a) a homogeneous fluid, (b) a vertically stratified fluid, and (c) a homogeneous fluid between two horizontal walls at $z = \pm 0.5$. Black lines are streamlines, colors show the logarithm of the magnitude of vertical velocity, w. Red dots in (b) show the location of the first zero crossing of w along the coordinate axes. The point force acts at the origin in all cases.
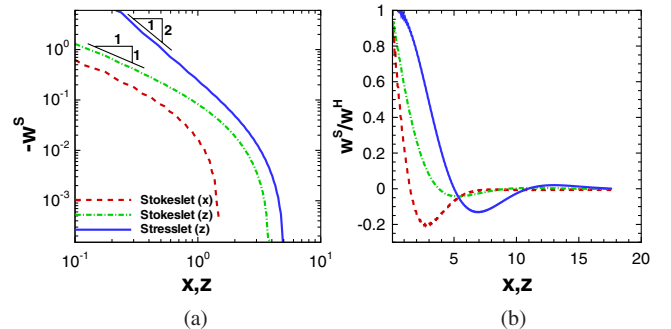

FIG. 2 (color online).   Vertical velocity w^S along the horizontal axis x (red dashed line) and the vertical axis z (green dashed-dotted line) for a vertical Stokeslet. Also shown is the vertical variation of w^S for a puller stresslet parallel to stratification (blue solid line). (a) Log-log plot; (b) linear plot, with w^S normalized by its homogeneous counterpart, w^H.
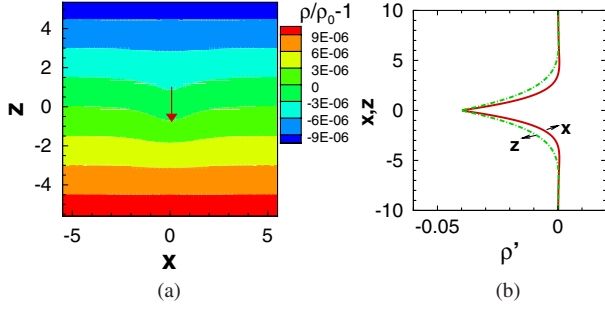
FIG. 3 (color online). Effect of a vertical Stokeslet on the density field. (a) Density contours $\rho/\rho_0 - 1 = -\gamma L z/\rho_0 + |\mathbf{f}|\rho'/(\rho_0 g L^3)$ for $|\mathbf{f}|/(\rho_0 g L^3) = 5 \times 10^{-5}$ and $\gamma L/\rho_0 = 2 \times 10^{-6}$. (b) Density perturbation ρ' along x and z.

The point force also deflects isopycnals, as shown by the contours of the density field [Fig. 3(a)]. The density perturbation ρ' is everywhere negative [Fig. 3(b)], since the point force draws lighter fluid from above into heavier fluid below. Isopycnal deflection is mild because of the smallness of the point force relative to the buoyancy force inherent in the linearization of Eq. (3).

In contrast to the homogeneous case, stratification breaks symmetry and the flow field of a stratified Stokeslet depends on the orientation of the point force relative to the stratification. When the two are not parallel, axisymmetry is lost. When they are perpendicular [Fig. 4(b)], no eddies form and fluid is simply pumped along the direction of the point force, as in the homogeneous case [Fig. 4(a)]. However, in contrast to the latter, vertical motion is again strongly inhibited by buoyancy and confined to the region closest to the point force, whereas flow is horizontal elsewhere.

The flow field induced by a swimming microorganism can be modeled to first order by a stresslet. Akin to the homogeneous case, we obtained the flow field of a stratified stresslet as the symmetric part of the stratified Stokes doublet, $\mathbf{u}^S_{\text{Doublet}} = -\beta \cdot \nabla \mathbf{u}^S_{\text{Stokeslet}}$. We computed the gradient numerically and used the same nondimensionalization as above, except for the velocity scale ($|\mathbf{f}||\beta|/(\mu L^2)$). We can distinguish two cases. Microorganisms can be "pullers" or "pushers", depending on whether they generate thrust in front or behind their body, relative to the direction of motion. Spermatozoa and bacteria have flagella behind the cell and thus are pushers, whereas algae like *Chlamydomonas* are pullers because flagella are in the front. For pushers, $\mathbf{f}$ and β are parallel, while for pullers they are antiparallel.

The velocity field of a vertically swimming puller (Fig. 5) is strikingly different in homogeneous and stratified fluids. In a homogeneous fluid, velocity is purely radial [Fig. 5(a) and [3]] and decays like $1/r^2$ [Fig. 2(a) for $z \to 0$]. In contrast, a puller in a stratified fluid generates two counter-rotating toroidal eddies, which drive additional ones further afield. The vertical extent of the main eddies is 5. Furthermore, velocity decays faster than $1/r^2$ [Fig. 2(a)]. The increase in decay rate compared to the
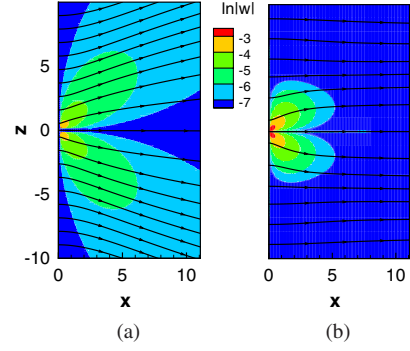

FIG. 4 (color online). Flow induced by a horizontal point force (Stokeslet) acting at the origin in (a) a homogeneous fluid, and (b) a vertically stratified fluid.

homogeneous case, quantified by w^S/w^H [Fig. 2(b)], is less than for the Stokeslet, yet still considerable, with w^S dropping to zero at $z = 5$. Isopycnals (not shown) reveal that a puller locally enhances stratification by pulling fluid in from above and below and expelling it laterally. This results in a net sharpening of the local density gradient. A pusher does the opposite.

Whether stratification affects the flow field generated by an object of a given size, a, can be predicted with the Rayleigh number, Ra. If one uses a rather than L in the nondimensionalization, then results depend on Ra $= (a/L)^4 = a^4 \gamma g/\mu\kappa$, which measures the relative importance of buoyancy and diffusion. Thus, the importance of stratification is assessed by comparing the scale of the object with the fundamental length scale of a stratified, diffusive fluid (and not with ρ_0/γ). When Ra $\geq O(1)$, the effect of stratification is significant.

Let us consider some examples. In salt-stratified water ($\kappa \approx 10^{-9}$ m^2 s^{-1}, $\mu \approx 10^{-3}$ kg m^{-1} s^{-1}) with $\gamma = 1$ kg m^{-4}, $L = 560$ μm. In temperature-stratified water ($\kappa \approx 10^{-7}$ m^2 s^{-1}), the same density gradient γ gives $L = 1.8$ mm. Thus, even objects that are $O(100 \mu$m $- 1$ mm) in size are affected by stratification, in stark contrast to what one would predict based on ρ_0/γ. The weak dependence of L on κ implies that stratification effects are rather similar in freshwater (typically temperature-stratified) and marine environments
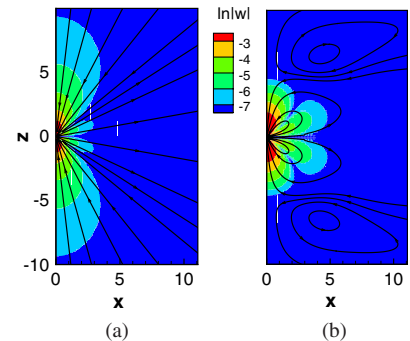

FIG. 5 (color online). Flow induced by a vertical puller stresslet acting at the origin in (a) a homogenous fluid, and (b) a vertically stratified fluid.

(often salt-stratified). Bacteria (~1 μm), phytoplankton (~10–100 μm), microparticles (<1–100 μm), and microzooplankton (~2–200 μm) will largely be unaffected. In contrast, marine snow (>0.5 mm), larger pellets (~0.2–2 mm), copepods (~0.5–3 mm), and small fish larvae (~5–20 mm) are of the same order or larger than L. Their Ra can thus exceed one and the flow they generate can be significantly affected by stratification.

The dramatic change in the flow field caused by stratification can have widespread ecological consequences. First, it can alter the exchange of solutes, including the leakage of dissolved organic matter by sinking particles and the nutrient uptake by organisms [11]. Second, it can modify recruitment rates of small particulates, e.g., bacterial attachment to marine snow or prey capture by suspension feeders [11]. Third, it can affect predator-prey interactions by reducing hydromechanical signals, acting as a stealth mechanism for swimming prey or as a "silencer" for approaching predators [11].

We quantified the extent to which stratification reduces the flow signature of a moving organism by computing the volume V^S in which the stresslet velocity exceeds a threshold ($|\mathbf{u}| > 0.01$). We found $V^S/a^3 \approx 60\text{Ra}^{-3/4}$ and $V^S/V^H \approx 0.45\text{Ra}^{-3/4}$, where V^H is the homogeneous counterpart of V^S (the $\text{Ra}^{-3/4}$ scaling also applies if sensing is based on shear rather than velocity). For the above salt stratification, the detection volume is reduced by 45% for a 560 μm prey, suggesting a significant impact on predator-prey interactions. Similarly, it can be shown that the energy expended by a swimming organism ($\int_V(\tau:\nabla\mathbf{u} + \rho'gw)dV$, where $\tau = \mu(\nabla\mathbf{u} + \nabla\mathbf{u}^T)$ is the viscous stress) in a stratified fluid, normalized by the homogeneous case, scales with $\text{Ra}^{3/4}$, implying that swimming is energetically more expensive at pycnoclines. In the ocean, organisms and particles will further be exposed to local variations in stratification, caused, for example, by internal waves or turbulence. The current analysis would then apply to the local stratification, or represent a linear, mean effect.

It is important to stress that Stokeslet and stresslet are only first-order solutions to sinking particles and swimming organisms, respectively. Accurate description of particle settling requires numerical solution of the nonlinear equations [5]. For organisms, details of the morphology and appendage kinematics can be included by superposition of fundamental solutions, exploiting the linearity of the Stokes equation. This approach is the basis of slender-body theory and boundary integral methods, which have been broadly applied to ciliary and flagellar dynamics [12]. These superposition methods can be extended to Stratlets, after deriving solutions to higher-order singularities.

The current analysis is restricted to small point forces, hence weak density perturbations. In dimensional form, Eq. (4) is valid when $|\mathbf{u}\cdot\nabla\rho'| \ll |w\gamma|$. Since $\mathbf{u}$ and w scale similarly, this implies that $|\nabla\rho'| \ll \gamma$, i.e., the density perturbation gradient must be much smaller than the background stratification. In dimensionless form, this

amounts to $|\nabla\rho'| \ll (\gamma gL^4)/|\mathbf{f}|$. Since $|\nabla\rho'|$ is at most 0.04 [Fig. 3(b)], this requires a point force $|\mathbf{f}| \ll 25\gamma gL^4$. For a particle of size a moving with velocity U, $|\mathbf{f}|$ can be taken as equal to the drag force $6\pi\mu aU$, yielding a maximum sinking speed $Ua/\kappa \ll 1.3$. This amounts to requiring a small Peclet number, Ua/κ. For example for 2 mm objects in temperature-stratified water, the maximum sinking velocity is 0.07 mm s^{-1} and the maximum swimming speed is 0.02 mm s^{-1} for the linearization to hold. The fact that these speeds are on the smaller side of observed ones [4] implies even stronger changes in the flow field, the description of which requires solution of the nonlinear Eqs. (3).

A significant fraction of the biological activity in aquatic environments occurs at interfaces. Density interfaces are ubiquitous, represent partial barriers to the vertical propagation of living and nonliving matter [4,5], and can attract swimming organisms [13]. The solutions derived here suggest that they are also niches where hydromechanical signals are damped and the performance of mechanosensing organisms reduced. These results await and invite experimental verification.

Note added in proof.—During the production of this manuscript, Raymond Goldstein brought to our attention an article by E. J. List [14], which has partial overlap with the solution discussed here. Where overlap exists, the results from the two studies are in agreement.

[1] G. Taylor, Proc. R. Soc. A **209**, 447 (1951).
[2] J. Lighthill, SIAM Rev. **18**, 161 (1976).
[3] A. T. Chwang and T. Y. T. Wu, J. Fluid Mech. **67**, 787 (1975).
[4] S. MacIntyre, A. L. Alldredge, and C. C. Gotschalk, Limnology and Oceanography **40**, 449 (1995).
[5] K. Y. Yick, C. R. Torres, T. Peacock, and R. Stocker, J. Fluid Mech. **632**, 49 (2009).
[6] A. N. Srdic-Mitrovic, N. A. Mohamed, and H. J. S. Fernando, J. Fluid Mech. **381**, 175 (1999).
[7] J. S. Turner, *Buoyancy Effects in Fluids* (Cambridge University Press, Cambridge, England, 1973).
[8] O. M. Phillips, Deep-Sea Research **17**, 435 (1970).
[9] C. F. Chen, J. Fluid Mech. **72**, 721 (1975).
[10] N. Liron and J. R. Blake, J. Fluid Mech. **107**, 109 (1981).
[11] T. Kiørboe, *A Mechanistic Approach to Plankton Ecology* (Princeton Univ. Press, Princeton, NJ, 2008), p. 228.
[12] C. Brennen and H. Winet, Annu. Rev. Fluid Mech. **9**, 339 (1977).
[13] B. Bergstrom and J. O. Stromberg, J. Plankton Res. **19**, 255 (1997).
[14] E. J. List, J. Fluid Mech., **45**, 561 (1971).